Engineering functionality in the multiferroic $BiFeO_3$ – controlling chemistry to enable advanced applications

Lane W. Martin*

Received 30th May 2010, Accepted 12th July 2010
DOI: 10.1039/c0dt00576b

An in-depth look at the complex materials chemistry of multiferroics is undertaken. In the last decade, considerable attention has been focused on the search for and characterization of new multiferroic materials as scientists and researchers have been driven by the promise of exotic materials functionality (*i.e.*, electric field control of ferromagnetism). In this manuscript we develop a picture of multiferroic materials, including details on the nature of order parameters and coupling in these materials, the scarcity of such materials, routes to create and control the properties in these materials, and we finish by investigating such effects in the model multiferroic $BiFeO_3$.

Introduction

Complex oxides represent a vast class of materials encompassing a wide range of crystal structures and functionalities. Amongst these interesting properties, the study of magnetic, ferroelectric, and, more recently, multiferroic properties in these oxide materials has driven considerable research. Specifically, in the last few years there has been a flurry of research focused on multiferroic and magnetoelectric materials.[1–3] From the investigation of bulk single crystals to novel characterization techniques that probe order parameters, coupling, spin dynamics, and more, this is truly a diverse field, rich with experimental and theoretical complexity. By definition, a single phase multiferroic[4] is a material that simultaneously possesses two or more of the so-called "ferroic" order parameters – ferroelectricity, ferromagnetism and ferroelasticity. Magnetoelectric coupling typically refers to the linear magnetoelectric effect or the induction of magnetization by an electric field or polarization by a magnetic field.[5] The promise of coupling between magnetic and electronic order parameters and the potential to manipulate one through the other has captured the imagination of researchers worldwide. The ultimate goal for device functionality would be a single phase multiferroic with strong coupling between ferroelectric and ferromagnetic order parameters making for simple control over the magnetic nature of the material with an applied electric field at room temperature.

One aspect of fundamental interest to the study of multiferroics is the production of high quality samples of such materials for detailed study. Previous reviews have focused on both bulk and thin film synthesis of these materials (for instance, ref. 6 and 7, respectively); however, in this perspective, we will discuss the basics of and fundamental nature of order parameters in multiferroics, and how this leads to a scarcity of candidate materials. We will proceed to discuss a number of different classes of multiferroics as well as the coupling between order parameters in these materials before finally focusing on the model multiferroic $BiFeO_3$ as an illustrative example of the successes and challenges in controlling the complex chemistries in these materials.

Department of Materials Science and Engineering and Frederick Seitz Materials Research Laboratory, University of Illinois, Urbana-Champaign, Urbana, IL 61801, USA

Prof. Lane W. Martin

Prof. Lane W. Martin is an Assistant Professor in the Department of Materials Science and Engineering at the University of Illinois, Urbana-Champaign. He obtained his B.S. degree from Carnegie Mellon University in December 2003 and his M.S. and Ph.D. degrees in Materials Science and Engineering from the University of California, Berkeley in May 2006 and March 2008, respectively. He worked as a post-doctoral fellow at Lawrence Berkeley National Laboratory from March 2008 to July 2009. Martin's research focuses on the growth and characterization of novel oxide materials in pursuit of two major research thrusts: multiferroic and multifunctional materials and devices and energy applications.

Multiferroic materials and scarcity

Multiferroism describes materials in which two or all three of the properties ferroelectricity (spontaneous polarization that is both stable and can be switched by application of an electric field), ferromagnetism (spontaneous magnetization that is stable and can be switched by application of a magnetic field), and ferroelasticity (spontaneous deformation that is stable and can be switched by application of an electric field) occur in the same phase. The overlap required of ferroic materials to be classified as *multiferroic* is shown schematically in Fig. 1(a). Only a small subgroup of all magnetically and electrically polarizable materials are either ferromagnetic or ferroelectric and fewer still simultaneously exhibit both order parameters. In these select materials, however, there is the possibility that electric fields cannot only reorient the polarization but also control magnetization; similarly, a magnetic field can change electric polarization. This functionality offers an extra degree of freedom and hence we refer to such materials as *magnetoelectrics* [Fig. 1(b)]. Magnetoelectricity is an independent phenomenon that can arise in any material with both magnetic and

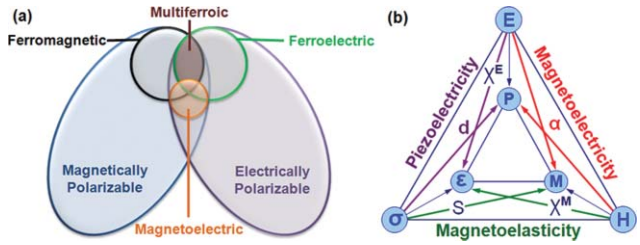

Fig. 1 (a) Relationship between multiferroic and magnetoelectric materials illustrating the requirements to achieve both in a material (adapted from ref. 8). (b) Schematic illustrating different types of coupling present in materials. Much attention has been given to materials where electric and magnetic order is coupled. These materials are known as magnetoelectric materials (adapted from ref. 7).

electronic polarizability, regardless of whether it is multiferroic or not. By the original definition a magnetoelectric multiferroic must be simultaneously both ferromagnetic and ferroelectric,[4] but it should be noted that the current trend is to extend the definition of multiferroics to include materials possessing two or more of any of the ferroic or corresponding antiferroic properties such as antiferroelectricity (possessing ordered dipole moments that are aligned antiparallel and therefore cancel each other completely across the sample) and antiferromagnetism (possessing ordered magnetic moments that are aligned antiparallel and therefore cancel each other completely across the sample). More recently it has also been extended to include so called ferrotoroidic order (a spontaneous order parameter that is taken to be the curl of a magnetization or polarization).[8] This said, it should be abundantly obvious why there has been considerable renewed interest in these materials over the last decade. The prospects for these materials in applications are wide ranging and have driven a dearth of both fundamental and applied studies. Multiferroics have been proposed for use in applications ranging from next generation logic and memory to sensing to tunable RF and much more. Although we will not explicitly explore these various applications, it is important to frame the following discussion in the context of the actual applications that are envisioned for these materials.

With this as a background, the single largest limiting factor that has kept multiferroics from making substantial in-roads into the current technology is the scarcity of multiferroics. This scarcity has been astutely demonstrated by Khomskii.[9] Taking as an example the perovskite (ABO_3) compounds, one can obtain a detailed list of magnetic perovskites in the tables compiled by Goodenough and Longo[10] and further investigation will reveal similar tables of ferroelectric perovskites complied by Mitsui, *et al.*[11] What becomes apparent after investigating these tables is that there is essentially no overlap between these lists – magnetism and ferroelectricity in the perovskites are seemingly incompatible. Key insights into this scarcity of multiferroic phases can be understood by investigating a number of factors including symmetry, electronic properties, and chemistry.[12,13] To begin, it should be noted that there are only 13 point groups that can give rise to multiferroic behavior. Strong magnetism in itinerant ferromagnets requires the presence of conduction electrons in partially filled inner shells (*d*- or *f*-shells); even in double exchange ferromagnets such as the manganites, magnetism is mediated by incompletely filled 3d shells. The situation in ferroelectrics, however, is somewhat more complicated as there exist many different mechanisms for ferroelectric ordering and a number of different types of ferroelectrics. Generally it is observed, however, that ferroelectrics (which are by definition insulators) typically possess, for instance in transition metal oxides, cations that have a formal d^0 electronic state. This d^0 state is thought to be required to drive the formation of strong covalency with the surrounding oxygen, thereby, shifting the transition metal ion from the center of the unit cell and inducing a spontaneous polarization (this is the so-called second-order Jahn–Teller effect).[14] The second-order Jahn–Teller effect describes the structural changes resulting from a nondegenerate ground-state interacting with a low-lying excited state and it occurs when the energy gap between the highest occupied (HOMO) and lowest unoccupied (LUMO) molecular orbital is small and there is a symmetry allowed distortion permitting the mixing of the HOMO and LUMO states. Mathematically, the second-order Jahn–Teller effect can be understood through the use of second-order perturbation and group theory, but this is beyond the scope of this article.[15] Thus, in the end, it becomes clear that there exists a seeming contradiction between the conventional mechanism of off-centering in a ferroelectric and the formation of magnetic order which helps explain the scarcity of ferromagnetic-ferroelectric multiferroics. The focus of many researchers, therefore, has been in designing and identifying new mechanisms that lead to magnetoelectric coupling and multiferroic behavior. In the following section we will investigate a number of these pathways.

An investigation of these various pathways to multiferroism is aided by separation of all multiferroic materials into one of two types.[16] Type I multiferroics are materials in which ferroelectricity and magnetism have different sources and appear largely independent of one another. One can create a Type I multiferroic, for instance, by engineering the functionality on a site-by-site basis in model systems such as the perovskites (ABO_3) where one can make use of the stereochemical activity of an A-site cation with a lone pair (*i.e.*, 6*s* electrons in Bi or Pb) to induce a structural distortion and ferroelectricity while inducing magnetism with the B-site cation. This is the case in the multiferroics $BiFeO_3$,[17] $BiMnO_3$,[18,19] and $PbVO_3$.[20–23] From the microscopic view, it can be understood that the orientation of the lone-pairs in the materials can give rise to local dipoles that can order thereby creating a net polarization as has been demonstrated with *ab initio* models (Fig. 2).[24] Much like the polarization observed in the classic ferroelectrics (*i.e.*, $BaTiO_3$), materials such as $BiFeO_3$ and $BiMnO_3$ are referred to as *proper* ferroelectrics. In a proper ferroelectric, structural instability towards a polar state, associated with the electronic pairing, is the main driving force for the transition. If, on the other hand, polarization is only a part of a more complex lattice distortion or if it appears as an accidental by-product of some other ordering, the ferroelectricity is called *improper*.[25] One pathway by which one can obtain an improper ferroelectric, Type I multiferroic is through geometrically driven effects where long-range dipole–dipole interactions and anion rotations drive the system towards a stable ferroelectric state. This is thought to drive multiferroism in materials such as the hexagonal manganites (*e.g.*, $YMnO_3$) (Fig. 3).[26,27] Again, in these materials ferroelectricity is achieved despite violating the requirement of having a d^0 electron configuration on the B-site cation. Despite this fact, the resulting ferroelectric transition temperatures for these hexagonal manganites are typically quite high (~900–1000 K) – suggesting a robustness to the order parameter. Recent results also suggest that

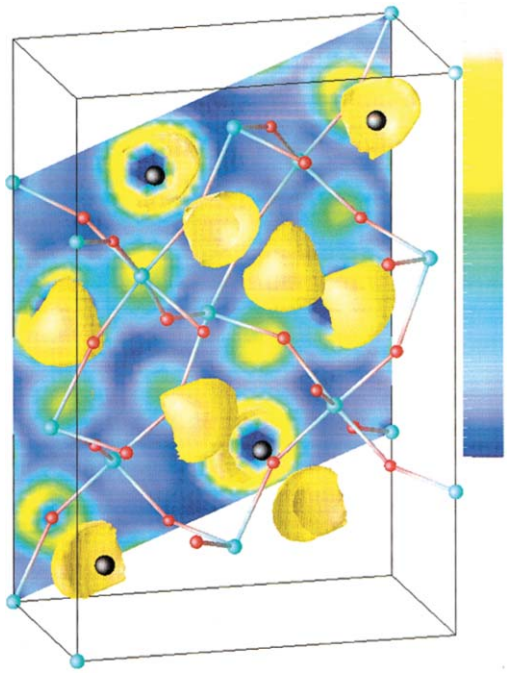

Fig. 2 Electron localization function representation of the isosurface of the valence electrons in $BiMnO_3$ projected within a unit cell. Blue colors correspond to a lack of electron localization and white to complete localization (adapted from ref. 24).

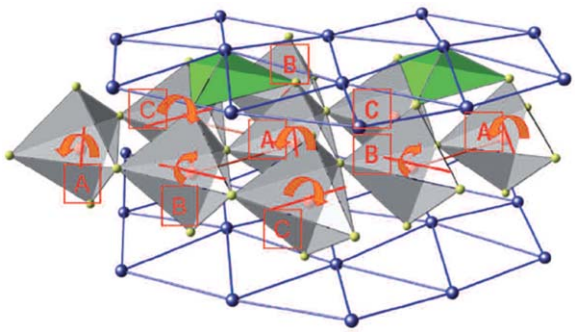

Fig. 3 Schematic illustration of the cooperative rotation of bipyramids in $YMnO_3$ that give rise to ferroelectric polarization. Oxygen ions are shown in yellow, Y ions in blue, and Mn ions in red. The resulting rotations are shown with the arrows (adapted from ref. 27).

the off-center shift of the Mn^{3+} ions (which, it should be noted, are not Jahn–Teller ions) from the center of the O_5 trigonal biprism are quite small and are, in turn, not the major mechanism for ferroelectric order in the system. Instead it is thought that the main dipole moments are formed (for instance in $YMnO_3$) by the Y–O pairs – thus suggesting that the mechanism of ferroelectricity in these materials is distinctly different from that observed in classic ferroelectric materials such as $BaTiO_3$.[26] Still another pathway by which one can achieve improper ferroelectricity in a Type I multiferroic is *via* charge ordering where non-centrosymmetric charge ordering arrangements result in ferroelectricity in magnetic materials as is found, for instance, in $LuFe_2O_4$.[28] It has long been known that in many narrowband metals with strong electronic correlations, charge carriers become localized at low temperatures and form periodic superstructures. The most famous example is magnetite (Fe_3O_4), which undergoes a metal–insulator transition at ~125 K (the Verwey transition) with a rather complex pattern of ordered charges of iron ions.[29] This charge ordering (which occurs in a non-symmetric manner) induces an electric polarization. More recently it has been suggested that the coexistence of bond-centered and site-centered charge ordering in $Pr_{1-x}Ca_xMnO_3$ leads to a non-centrosymmetric charge distribution and a net electric polarization [Fig. 4(a)].[30] In the case of $LuFe_2O_4$, the charge ordering results in a bilayer structure and appears to induce electric polarization. The average valence of Fe ions in $LuFe_2O_4$ is 2.5+, and in each layer these ions form a triangular lattice. Below ~350 K, it is thought that alternating layers with $Fe^{2+}:Fe^{3+}$ ratios of 2 : 1 and 1 : 2 are produced, which result in a net polarization [Fig. 4(b)].[28]

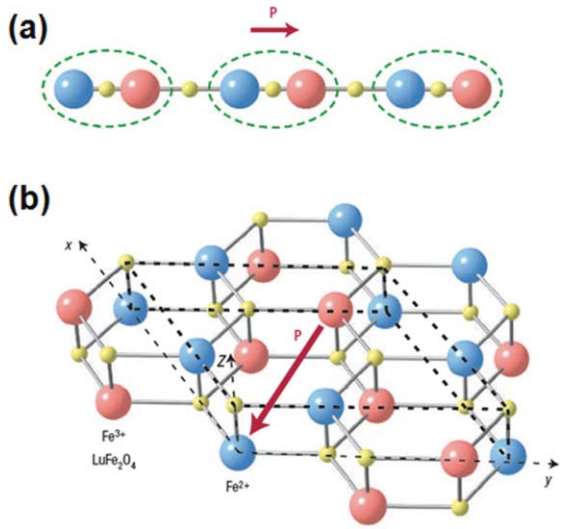

Fig. 4 (a) Illustration describing how ferroelectric order can be achieved in charge-ordered systems. Red/blue spheres correspond to cations with more/less charge and ferroelectricity is induced by the presence of simultaneous site-centered and bound-centered charge ordering. Dimers are marked by the dashed green lines. (b) Charge ordering in $LuFe_2O_4$ with a triangular lattice of Fe-ions in each layer – charge transfer from the top to bottom layer gives rise to a net electric polarization (adapted from ref. 2).

So far we have investigated Type I multiferroics, where magnetism and ferroelectricity result from two unrelated mechanisms. In these systems because the ordering results from very different mechanisms, one would not, *a priori*, expect there to be strong magnetoelectric coupling in these materials. On the other hand, Type II multiferroics are materials in which magnetism causes ferroelectricity – implying a strong coupling between the two order parameters. The prototypical examples of this sort of behavior are $TbMnO_3$[31] and $TbMn_2O_5$[32] where ferroelectricity is induced by the formation of a symmetry-lowering magnetic ground state that lacks inversion symmetry. For instance, in $TbMnO_3$, the onset of ferroelectricity is directly correlated with the onset of spiral magnetic order at ~28 K.[33] The intimate connection between magnetic and ferroelectric order results in extraordinary coupling – including the ability to change the direction of electric polarization with an applied magnetic field in $TbMnO_3$[31] and switching from positive to negative polarization in $TbMn_2O_5$ with a magnetic field.[32] The true nature of the mechanism for ferroelectric ordering

in these materials is still under debate. Current theories have noted that for most of these materials the ferroelectric state is observed only when there is a spiral or helicoidal magnetic structure. The idea is that *via* some mechanism, for instance the Dzyaloshinskii–Moriya antisymmetric exchange interaction[34,35] which is a relativistic correction to the usual superexchange with strength proportional to the spin–orbit coupling constant, the magnetic spiral can exert an influence on the charge and lattice subsystems, thereby creating ferroelectric order. Similar effects have also been observed in $Ni_3V_2O_8$.[36]

Magnetoelectricity

From an applications standpoint, the real interest in multiferroic materials lies in the possibility of strong magnetoelectric coupling and the possibility to create new functionalities in materials. The magnetoelectric effect was proposed as early as 1894 by P. Curie,[37] but experimental confirmation of the effect remained elusive until work on Cr_2O_3 in the 1960s.[38,39] As early as the 1970s a wide range of devices, including devices for the modulation of amplitudes, polarizations, and phases of optical waves, magnetoelectric data storage and switching, optical diodes, spin-wave generation, amplification, and frequency conversion had been proposed that would take advantage of magnetoelectric materials.[40] The magnetoelectric effect in its most general definition delineates the coupling between electric and magnetic fields in matter. Magnetoelectric coupling may exist regardless of the nature of the magnetic and electrical order parameters and can arise from direct coupling between two order parameters or indirectly *via* the lattice or strain. A better understanding of magnetoelectric coupling arises from expansion of the free energy of a material, *i.e.*

$$F(\vec{E},\vec{H}) = F_0 - P_i^S E_i - M_i^S H_i - \frac{1}{2}\varepsilon_0\varepsilon_{ij}E_iE_j - \frac{1}{2}\mu_0\mu_{ij}H_iH_j - \frac{1}{2}\beta_{ijk}E_iH_jH_k - \frac{1}{2}\gamma_{ijk}HiE_jE_k - \ldots \quad (1)$$

with $\vec{E}$ and $\vec{H}$ as the electric field and magnetic field, respectively. Differentiation leads to the constitutive order parameters polarization

$$P_i(\vec{E},\vec{H}) = \frac{\partial F}{\partial E_i} = P_i^S + \varepsilon_0\varepsilon_{ij}E_j + \alpha_{ij}H_j + \frac{1}{2}\beta_{ijk}H_jH_k + \gamma_{ijk}H_iE_j + \ldots \quad (2)$$

and magnetization

$$M_i(\vec{E},\vec{H}) = -\frac{\partial F}{\partial E_i} = M_i^S + \mu_0\mu_{ij}H_j + \alpha_{ij}E_i + \beta_{ijk}E_iH_j + \frac{1}{2}\gamma_{ijk}E_jE_k + \ldots \quad (3)$$

where ε and μ are the electric and magnetic susceptibilities, respectively, and α represents the induction of polarization by a magnetic field or magnetization by electric field and is designated the linear magnetoelectric effect. It should be noted that higher order magnetoelectric effects like β and γ are possible, however, they are often much smaller in magnitude then the lowest order terms. Furthermore, it can be shown that the magnetoelectric response is limited by the relation $\alpha_{ij}^2 < \varepsilon_{ii}\mu_{jj}$ or more rigorously $\alpha_{ij}^2 < \chi_{ii}^{e}\chi_{jj}^{e}$ where χ^e and χ^m are the electric and magnetic susceptibilities. This means that the magnetoelectric effect can only be large in ferroelectric and/or ferromagnetic materials. To date the largest magnetoelectric responses have been identified in composite materials where the magnetoelectric effect is the product property of a magnetostrictive and a piezoelectric material and in multiferroic materials.[41]

Symmetry also has a key role to play in magnetoelectricity. In fact, Curie's early work had already pointed to the fact that symmetry was a key issue in the search for magnetoelectric materials, but it was not until much later that researchers realized magnetoelectric responses could only occur in time-asymmetric materials.[42] Detailed symmetry analyses[43–45] have produced lists of magnetoelectric point groups and tensor elements. By definition the magnetoelectric effect involves both magnetic and electric fields, thereby ruling out materials with either time reversal or inversion symmetry. In the end there are only 58 magnetic point groups that allow the magnetoelectric effect. These symmetry concerns have lead to a strict set of criteria that must be met for a material to exhibit magnetoelectric behavior.

Modern-Day multiferroics

Multiferroics have a storied history dating back to the 1950s. At that time, Soviet scientists attempted to replace partially diamagnetic ions with paramagnetic ones on the B-site of oxy-octahedral perovskites[46,47] making the phases $Pb(Fe_{1/2}Nb_{1/2})O_3$ and $Pb(Fe_{1/2}Ta_{1/2})O_3$ which were found to be both ferroelectric and antiferromagnetic. This sparked the birth of the field of multiferroics. Following this initial period of interest throughout the 1960s and 1970s, these materials were relegated to the realms of physics novelty as the complex nature of these materials made it quite difficult to produce high quality materials that possessed the desired combination of properties. The so-called "Renaissance of Magnetoelectric Multiferroics"[48] came in the early 2000s as combined advances in the production of high quality thin films and bulk single crystals were augmented by significant advances in materials characterization (especially scanning probe, optical, neutron, and synchrotron-based techniques) made it, for the first time, possible to synthesize high quality samples and characterize multiple order parameters in these materials.

Today there are roughly four major classes of multiferroic materials: (1) materials with the perovskite structure, (2) materials with hexagonal structure, (3) boracites, and (4) $BaMF_4$ compounds. Briefly we will investigate each of these classes of multiferroics before proceeding to focus on one major example. Let us begin at the end of the list by investigating multiferroics with $BaMF_4$ (M = Mg, Mn, Fe, Co, Ni and Zn) structure. These materials have been studied since the late 1960s and are typically defined by their orthorhombic structure and 2*mm* point group symmetry.[49,50] Often their extrapolated Curie temperatures are very high (in excess of the melting point) and at low temperatures (<100 K) the ferroelastic, ferroelectric structure exhibits antiferromagnetic or weakly ferromagnetic order.[51] Moving on to some of the other common multiferroic structures, the boracites, with general chemical formula $M_3B_7O_{13}X$ (M = Cr, Mn, Fe, Co, Cu, Ni; X = Cl, Br), are typically ferroelastic ferroelectric, antiferromagnets (and occasionally weakly ferromagnetic). In some cases the ferroelectric Curie temperature can exceed room temperature, but (again) the magnetic ordering temperatures are generally less than 100 K.[51] The materials undergo a classic transition from a

high-temperature cubic phase ($\bar{4}3m$ symmetry)[52] at high temperatures to an orthorhombic structure ($mm2$ symmetry). Note that some phases also possess subsequent phase transitions to m and $3m$ symmetry at lower temperatures.[53,54] The third common class of multiferroic materials are those possessing hexagonal structure and general chemical formula ABO_3 or $A_2B'B''O_6$. Of these materials, the best known and studied are the hexagonal ferroelectric, antiferromagnetic manganites ($RMnO_3$, R = Sc, Y, In, Ho, Er, Tm, Yb, Lu) which were first discovered in the late 1950s.[55,56] These materials are defined by $6mm$ symmetry and up to four long-range ordered subsystems, including the ferroelectric lattice with Curie temperatures typically between 570–990 K,[51,56] the antiferromagnetic Mn^{3+} lattice with Néel temperatures typically between 70–130 K,[57] and two rare-earth sublattices with magnetic order temperatures below ~5 K.[58] This brings us to the oldest and best known class of multiferroic materials that are based on the perovskite structure with general chemical formula ABO_3, $A_2B'B''O_6$, or a large variety of doped or chemically substituted phases. Generally multiferroic perovskites do not possess ideal cubic symmetry ($m3m$), but have some slight deformation (*i.e.*, a rhombohedral distortion as is the case in $BiFeO_3$ which has $3m$ symmetry). There are a large number of multiferroic perovskites (for a nice listing see ref. 51), but by far the most widely studied material has been $BiFeO_3$. Bismuth ferrite or $BiFeO_3$ is a ferroelastic ferroelectric, antiferromagnet with high ordering temperatures and can be chemically alloyed to tune the properties. Because of the versatility of this material, the high ordering temperatures, and the robust order parameters, it has attracted unprecedented attention since the first half of the 2000s. Thus, for the remainder of this manuscript, we will focus in on the evolution and properties of this exciting material.

$BiFeO_3$

The perovskite $BiFeO_3$ was first produced in the late 1950s[59] and many of the early studies were focused on the same concepts important today – the potential for magnetoelectric coupling.[60] Throughout the 1960s and 1970s much controversy surrounded the true physical and structural properties of $BiFeO_3$, but as early as the 1960s $BiFeO_3$ was suspected to be an antiferromagnetic, ferroelectric multiferroic.[61,62] The true ferroelectric nature of $BiFeO_3$, however, remained somewhat in question until ferroelectric measurements made at 77 K in 1970[62] revealed a spontaneous polarization of ~6.1 μC cm^{-2} along the 111-direction which were found to be consistent with the rhombohedral polar space group $R3c$ determined from single-crystal X-ray diffraction[63] and neutron diffraction studies.[64] These findings were at last confirmed by detailed structural characterization of ferroelectric/ferroelastic monodomain single crystal samples of $BiFeO_3$ in the late 1980s.[60] Chemical etching experiments on ferroelastic single domains later proved without a doubt that the $BiFeO_3$ was indeed polar, putting to rest the hypothesis that $BiFeO_3$ might be antiferroelectric, and proved that the ferroelectric/ferroelastic phase was stable from 4 K to ~1103 K.[65] The structure of $BiFeO_3$ can be characterized by two distorted perovskite blocks connected along their body diagonal or the pseudocubic <111>, to build a rhombohedral unit cell [Fig. 5(a)]. In this structure the two oxygen octahedra of the cells connected along the <111> are rotated clockwise and counterclockwise around the <111> by ± 13.8(3)° and the Fe-ion is shifted by 0.135 Å along the same axis away from the oxygen octahedron center position. The ferroelectric state is realized by a large displacement of the Bi-ions relative to the FeO_6 octahedra [Fig. 5(a), (b) and (c)].[60,66]

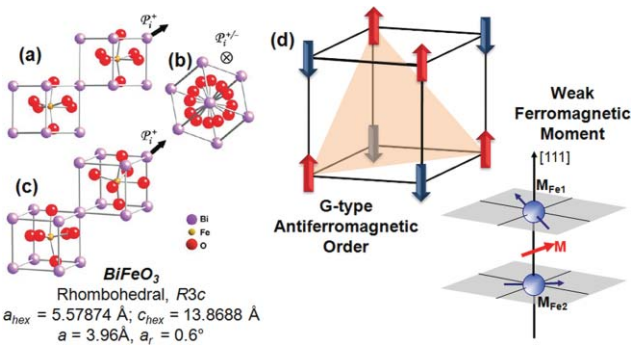

Fig. 5 Structure of $BiFeO_3$ shown looking (a) down the pseudocubic-[110], (b) down the pseudocubic-[111]-polarization direction, and (c) a general three-dimensional view of the structure (adapted from ref. 66). (d) The magnetic structure of $BiFeO_3$ is shown including G-type antiferromagnetic ordering and the formation of the weak ferromagnetic moment (adapted from ref. 7).

During the 1980s, the magnetic nature of $BiFeO_3$ was studied in detail. Early studies indicated that $BiFeO_3$ was a G-type antiferromagnet (G-type antiferromagnetic order is shown schematically in Fig. 5(d)) with a Néel temperature of ~673 K[67] and possessed a cycloidal spin structure with a period of ~620 Å.[68] This spin structure was found to be incommensurate with the structural lattice and was superimposed on the antiferromagnetic order. It was also noted that if the moments were oriented perpendicular to the <111>-polarization direction, the symmetry also permits a small canting of the moments in the structure, resulting in a weak ferromagnetic moment of the Dzyaloshinskii–Moriya type [Fig. 5(d)].[34,35]

In 2003 a paper focusing on the growth and properties of thin films of $BiFeO_3$ spawned a hailstorm of research into thin films of $BiFeO_3$ that continues to the present day. The paper reported enhancements of polarization and related properties in heteroepitaxially constrained thin films of $BiFeO_3$.[17] Structural analysis of the films suggested differences between films (with a monoclinic structure) and bulk single crystals (with a rhombohedral structure) as well as enhancement of the polarization up to ~90 μC cm^{-2} at room temperature and enhanced thickness-dependent magnetism compared to bulk samples (Fig. 6). In reality, the high values of polarization observed actually represented the intrinsic polarization of $BiFeO_3$. Limitations in the quality of bulk crystals had kept researchers from observing such high polarization values until much later in bulk samples.[69] More importantly this report indicated a magnetoelectric coupling coefficient as high as 3 V cm^{-1} Oe at zero applied field.[17] A series of detailed first principles calculations utilizing the local spin-density approximation (LSDA) and LSDA+U methods helped shed light on the findings in this paper. Calculations of the spontaneous polarization in $BiFeO_3$ suggested a value between 90–100 μC cm^{-2} (consistent with those measured in 2003)[70] which have since been confirmed by many other experimental reports. Other theoretical treatments attempted to understand the nature of magnetism and

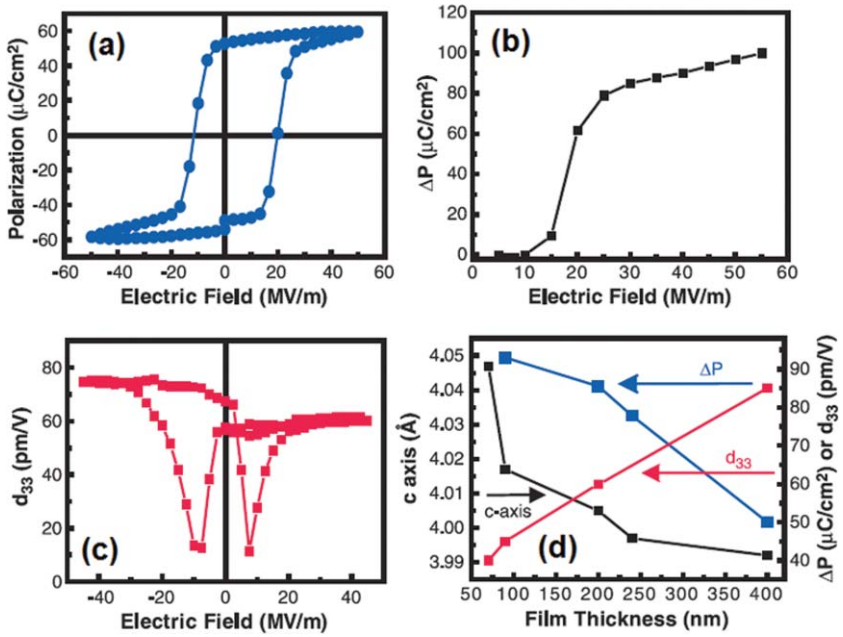

Fig. 6 (a) Ferroelectric polarization–electric field hysteresis loop of epitaxial $BiFeO_3$ thin film measured at 15 kHz. (b) Pulsed polarization (ΔP) *vs.* electric field measured with electrical pulses of 10 μs on the same $BiFeO_3$ film. (c) Piezoelectric response (d_{33}) for a 50 μm capacitor for the $BiFeO_3$ film. (d) Summary of thickness dependent evolution of out-of-plane lattice parameter, polarization, and d_{33} (adapted from ref. 17).

coupling between order parameters in $BiFeO_3$. Such calculations confirmed the possibility of weak ferromagnetism arising from a canting of the antiferromagnetic moments in $BiFeO_3$. The canting angle was calculated to be ~1° and would result in a small, but measurable, magnetization of ~0.05 μ_B per unit cell.[71] It was also found that the magnetization should be confined to an energetically degenerate easy {111} perpendicular to the polarization direction in $BiFeO_3$. These same calculations further discussed the connection of the weak ferromagnetism and the structure (and therefore ferroelectric nature) of $BiFeO_3$. This allowed the authors to extract three conditions necessary to achieve electric-field-induced magnetization reversal: (i) the rotational and polar distortions must be coupled; (ii) the degeneracy between different configurations of polarization and magnetization alignment must be broken; (iii) there must be only one easy magnetization axis in the (111) which could be easily achieved by straining the material.[71]

Nonetheless, the true nature of magnetism in thin film $BiFeO_3$ continues to be a contentious subject. The original work of Wang *et al.* presented an anomalously large value of magnetic moment (of the order of 70 emu cm^{-3}),[17] which is significantly higher than the expected canted moment of ~8 emu cm^{-3}. There have been several studies aimed at clarifying the origins of this anomalous magnetism. Eerenstein *et al.*[72] proposed that the excess magnetism was associated with magnetic second phases (such as γ-Fe_2O_3); this was supported by the studies of Béa *et al.*[73] who showed that $BiFeO_3$ films, when grown under reducing conditions (for example under oxygen pressures lower than 1×10^{-3} Torr) showed enhanced magnetism as a consequence of the formation of magnetic second phases. It is, however, important to note that low oxygen pressure during growth is not the cause for the enhanced moment in the 2003 report by Wang *et al.* where films were grown in oxygen pressures between 100–200 mTorr and cooled in 760 Torr rendering formation of such secondary magnetic phases thermodynamically unlikely and there was no evidence (despite extensive study of samples with X-ray diffraction and transmission electron microscopy techniques) for such second phases. Furthermore, subsequent X-ray magnetic circular dichroism studies supported the assertion that this magnetism is *not* from a magnetic γ-Fe_2O_3 impurity phase.[74] To date, additional mixed reports – including reports of enhanced magnetism in nanoparticles of $BiFeO_3$[75] as well as the observation of samples exhibiting no such enhancement – have been presented. It is thus fair to say that this one issue that remains unresolved in a rigorous sense.

Synthesis of $BiFeO_3$

Great strides have been made in the production of high quality bulk single-crystal and thin film versions of $BiFeO_3$ in the last few decades. Here will investigate the advances in each arena. Let us begin by investigating the development of bulk-single crystal synthesis. The creation of top-notch $BiFeO_3$ single crystals really finds its start in the mid 1980s in the group of Schmid at the University of Geneva and the use of the flux growth method to produce crystals.[76,77] Additional details concerning these growth techniques can be found in ref. 78 and 79. Briefly, the process generally uses Bi_2O_3/Fe_2O_3 flux with some additives to either promote single domain growth or lower liquidus temperatures (*i.e.*, B_2O_3, NaCl, *etc.*). Regardless, much of the early work fought the struggle against "parasitic" phases such as $Bi_2Fe_4O_9$ and others. The process requires careful control of the molar ratios of the starting materials, cooling rates, and gaseous environment. In the end the crystals must be separated from the flux *via* a number of different dissolution procedures (*i.e.*, using acetic, nitric or other acids). More recently the flux process has been evolved and currently very high quality single crystals of $BiFeO_3$ can

be produced using the flux process. Processes today still utilize the same basic Bi_2O_3/Fe_2O_3 flux in a Pt-crucible at temperatures between 675–870 °C,[80–82] various additions to promote single domain growth, and a better understanding of the common impurity phases and routes to avoid them are known. It is not uncommon for researchers today to achieve single crystal samples a few millimetres on a side (Fig. 7).

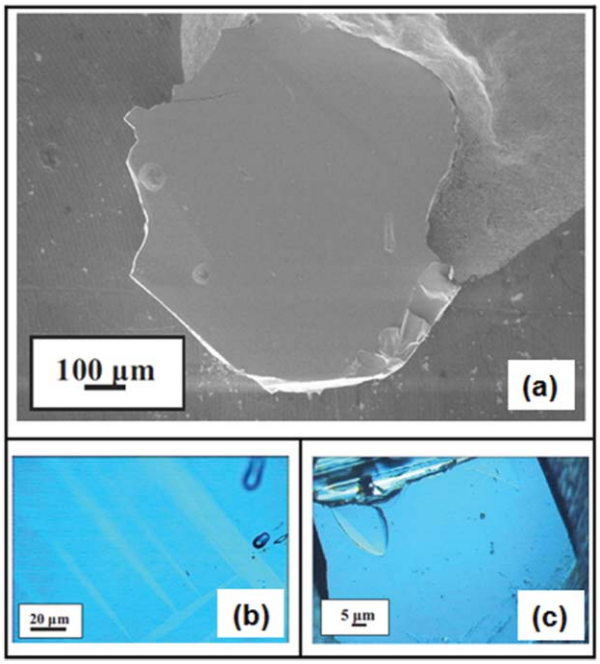

Fig. 7 (a) SEM image of a $BiFeO_3$ single crystal platelet grown from the flux method described. The crystal size is $1.4 \times 1.6 \times 0.04$ mm^3. (b) Imaged from a polarizing light microscope with a polychromatic light source showing the presence of different ferroelectric domains in the sample. (c) Similar images from another $BiFeO_3$ single crystal revealing the presence of only a single ferroelectric domain (adapted from ref. 69).

Although great strides have been made in the production of high quality single crystals of $BiFeO_3$, much of the research on this material has been driven by progress in understanding the structure, properties, and growth of thin films of $BiFeO_3$. High quality epitaxial $BiFeO_3$ films have been grown *via* molecular beam epitaxy (MBE),[83,84] pulsed laser deposition,[17,85] radio-frequency (RF) sputtering,[86,87] metalorganic chemical vapor deposition (MOCVD),[88,89] and chemical solution deposition (CSD)[90] on a wide range of substrates including traditional oxide substrates as well as Si[85,91] and GaN.[92] This work has shown that high quality films, like those shown in Fig. 8 can be produced. Typical XRD θ–2θ measurements [Fig. 8(a)] show the ability of researchers to produce high quality, fully epitaxial, single-phase films of $BiFeO_3$ (data here is for a $BiFeO_3/SrRuO_3/SrTiO_3$ (001) heterostructure). Detailed XRD analysis has shown that films possess a monoclinic distortion of the bulk rhombohedral structure over a wide range of thicknesses, but the true structure of very thin films (<15 nm) remains unclear.[93] The quality of such heterostructures as produced by pulsed laser deposition can be probed further by transmission electron microscopy (TEM) [Fig. 8(b)]. TEM imaging reveals films that are uniform over large areas and with the use of high-resolution TEM we can examine the atomically abrupt, smooth, and coherent interface between $BiFeO_3$ and a commonly used bottom electrode material $SrRuO_3$.

Epitaxy has allowed researchers to gain control over the complex domain structures common to $BiFeO_3$, which is especially important if one would like to control and influence the physical properties of these materials. A complete discussion of controlling domain structures in $BiFeO_3$ is given in ref. 3, but here are a few important findings. Researchers have been able to produce one-dimensional nanoscale arrays of domain walls in epitaxial BFO films by utilizing anisotropic in-plane strains,[94] reduce the structural variants from 8, to 4, to 2, and even a single variant through the use of vicinally cut substrates,[95] and by controlling the electrostatic boundary conditions researchers have been able to produce the equilibrium domain structures predicted nearly 10 years ago.[96,97] These advances in controlling the ferroelectric domain structure of $BiFeO_3$ show one way to improve the performance of such complex materials in device settings that could range from memories, to photonic devices, to nanolithography, and more. Such fine control of the domain structures (and, in turn, the properties) and the ability to create extremely high quality thin films of these materials make it possible to probe a number of important questions related to this material.

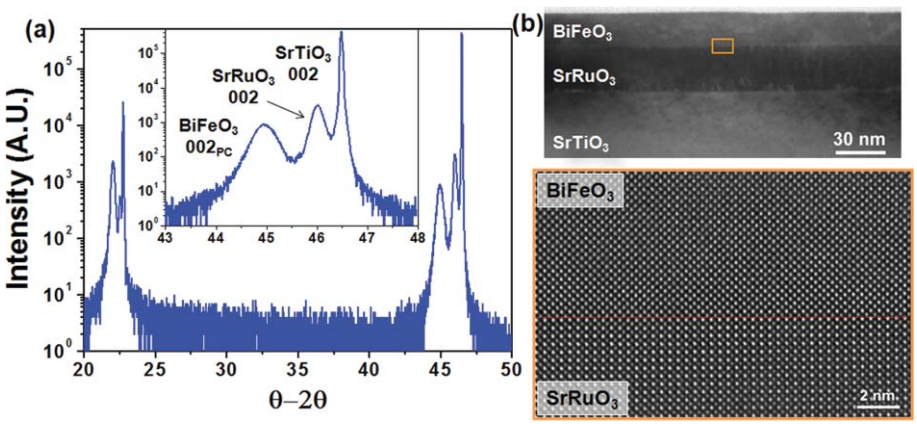

Fig. 8 (a) X-Ray diffraction results from a fully epitaxial, single phase $BiFeO_3/SrRuO_3/SrTiO_3$ (001) heterostructure. (b) Low- and high-resolution transmission electron microscopy images of this same heterostructure (adapted from ref. 7).

Doped $BiFeO_3$

In addition to improvements in the synthesis of $BiFeO_3$ thin films, other researchers have attempted to take head-on the common challenges that have traditionally limited the widespread usage of such materials in devices. These challenges have included high leakage currents, small remnant polarizations, high coercive fields, ferroelectric reliability, and inhomogeneous magnetic spin structures.[98] Specifically, in the last few years, attention has been given to studying doped $BiFeO_3$ thin films (both A-site and B-site doping) in an attempt to improve these various areas of concern. In this section we will describe the work done to date on chemical routes to control properties in $BiFeO_3$.

Following the rejuvenation of interest in $BiFeO_3$ in the early 2000s, a number of studies came forth aimed at understanding how to enhance properties in this exciting material. One of the earliest studies looked at alloying the B-site of $BiFeO_3$ with the transition metal ions Ti^{4+} and Ni^{2+} which are similar in size to the Fe^{3+} ion.[99] The idea was that the addition of 4+ ions into the $BiFeO_3$ would require charge compensation which would be achieved either by filling of oxygen vacancies, decreasing the valence of the Fe-ions, or creation of cation vacancies. On the other hand, addition of 2+ ions would likely create anion vacancies or change the Fe-ion valence. In the end the hope was that Ti^{4+} alloying would help to eliminate oxygen vacancies and Ni^{2+} alloying would introduce more oxygen vacancies. This study, in turn, showed that alloying with Ti^{4+} led to an increase in film resistivity by over three orders of magnitude while doping with Ni^{2+} resulted in a decrease in resistivity by over two orders of magnitude (Fig. 9). Additionally, the study suggested that the current–voltage behavior was effected by the alloying and that increased densities of oxygen vacancies lead to higher levels of free carriers and higher conductivity. Over the next few years numerous other reports of the effect of alloying on the properties of $BiFeO_3$ were published. Other studies also focused on B-site alloying, including alloying with Nd which helped to enhance piezoelectricity in the films and improve electric properties,[100,101] doping with Cr which was shown to greatly reduce leakage currents in $BiFeO_3$ films,[102] and others.

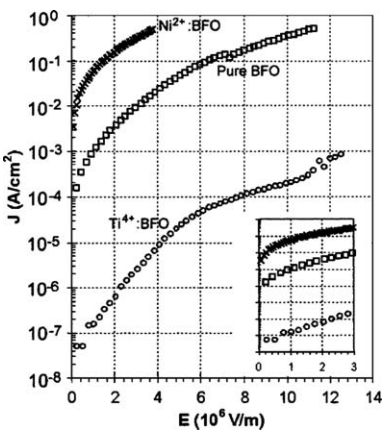

Fig. 9 Leakage current density as a function of applied electric field for pure and doped $BiFeO_3$ thin films. Ti-doped $BiFeO_3$ is shown to have significantly reduced leakage currents. Inset shows a zoom in of the low voltage region of the data (adapted from ref. 99).

Although there are a number of studies on B-site alloyed $BiFeO_3$, greater attention has been given to A-site alloyed phases. The most widely studied dopants are materials from the lanthanide series – especially La, Dy, Gd, *etc.* As early as 1991 work on these materials was undertaken,[103] but again it was not until after 2003 that the number of studies on these alloyed systems really took off. Early studies probed the effect of La-alloying on the magnetic structure of $BiFeO_3$ and showed that the spin-modulated structure disappeared in single crystals with only 20% addition of La.[104] Soon after, studies on La-alloyed thin films showed that the structure of the films was greatly affected, and that the ferroelectric fatigue life was seemingly enhanced.[98,105] Later studies showed that careful control of La-doping could be used to control domain structures, switching, and produce robust ferroelectric properties in films on Si substrates.[106] Other studies have also investigated Ba-,[107] Sr-, Ca- and Pb-doping,[108] and many others. It should be noted that there are numerous studies of A-site alloying, too many to be covered thoroughly here.

Another exciting discovery occurred when researchers doped rare-earth elements into $BiFeO_3$. Upon doping $BiFeO_3$ with Sm (at ~14% Sm), a lead-free morphotropic phase boundary was discovered.[109] The researchers found a rhombohedral to pseudo-orthorhombic structural transition (and an associated ferroelectric to antiferroelectric transition) that produced an out-of-plane piezoelectric coefficient comparable to $PbZr_xTi_{1-x}O_3$ materials near the chemically derived morphotropic phase boundary in that material. Further investigations of this morphotropic phase boundary have investigated the effects of Sm doping and have shown that the Sm^{3+} first creates antiparallel cation displacements in local pockets and, with additional Sm, a series of phase transitions and superstructural phases are formed.[110,111] This work has recently culminated in the observation of a universal behavior in such rare-earth substituted versions of $BiFeO_3$.[112] By combining careful experimental and first-principles approaches to the study of complex phase development in this system, researchers have discovered that the structural transition between a rhombohedral ferroelectric phase and an orthorhombic phase with a double-polarization hysteresis loop and significantly enhanced electromechanical response is found to occur independent of the rare-earth dopant species as long as the average ionic radius of the A-site cation is controlled. Despite the somewhat complicated phase space related to such doped versions of $BiFeO_3$, researchers have been able to identify and manipulate dopants to greatly enhance the properties of this material. It should also be noted at this point, that a recent report has suggested that thin film strain can be used to induce a similar morphotropic-like (or isosymmetric) phase boundary in $BiFeO_3$.[113] In this case a strain-driven boundary between a super-tetragonal-like and rhombohedral-like phase is observed. By utilizing epitaxial thin film strain, the authors of this report noted that growth of thin films on $LaAlO_3$ (001) and $YAlO_3$ (001) substrates resulted in the formation of $BiFeO_3$ exhibiting a nearly tetragonal polymorph of the typically rhombohedral material and the presence of mixed phase (possessing both rhombohedral- and tetragonal-like versions of $BiFeO_3$). Detailed transmission electron microscopy imaging of the interface between these two structural polymorphs showed that the *c*-axis lattice parameter changes by nearly 13% in only about 10 unit cells without the presence of misfit dislocations or other defects. Furthermore, initial findings suggest similar large piezoelectric

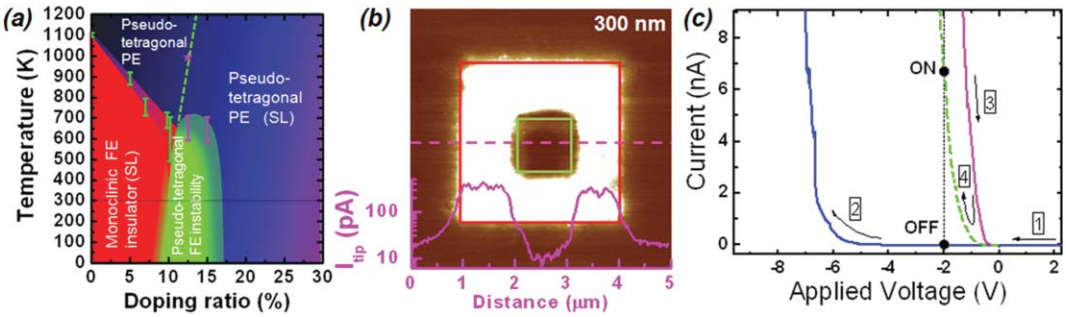

Fig. 10 (a) Pseudo-phase diagram of the evolution of structures and properties in Ca-doped $BiFeO_3$. (b) Conducting-atomic force microscopy image of an electrically poled and re-poled area of the a doped $BiFeO_3$ film. The as-grown state (outside the red box) is insulating in nature, the electrically poled area (inside the red box and outside the green box) has become conducting, and the area that has been electrically poled twice (inside green box) is insulating again. (c) Illustration of the process to create a multi-state memory from such physical properties (adapted from ref. 116).

coefficients are associated with this phase boundary. Scanning probed-based studies showed surface strains as large as 1.5% – similar to those observed in the traditional lead-based systems – and that one can electrically switch the material between a purely tetragonal-like phase and a mixture of rhombohedral- and tetragonal-like features. These mixed phases give rise to interesting stripe-like features on the surface of the samples. First-principles density functional theory studies of this phase boundary[114] have been presented that describe the evolution of this new behavior. Theory (and experiment) suggest that up until approximately 4% compressive strain (001)-oriented thin films experience little effect, but at this point increasing strain results in an isosymmetric phase transition and a dramatic change in structure. This structural transition is associated with a rotation of the polarization from the [111] to nearly the [001] and an increase in magnitude of nearly 50%. Finally, recent Raman and nanoscale studies of switching in these strain-engineered $BiFeO_3$ thin films have revealed that the tetragonal phase is likely to possess a slightly monoclinically distorted structure (*Cc*) rather than *P*4*mm* symmetry and, through the use of piezoresponse force microscopy, ferroelectric switching in the tetragonal-like phase was observed.[115] What becomes clear is that there are a number of routes by which one can achieve exotic new properties and functionality in systems such as $BiFeO_3$. From the use of rare-earth dopants to careful control of epitaxial strain, tweaking and tuning the structure and properties of these materials can result in unexpected findings.

The work in alloyed $BiFeO_3$ materials was undertaken with the expectation that this would present an exciting pathway to unprecedented control and properties in this material. The findings, although useful and insightfull, had failed to produce a ground breaking discovery until very recently. In 2009, Yang *et al.*,[116] building off of the prior observation of the development of interesting materials phenomena such as high-T_C superconductivity in the cuprates and colossal magnetoresistance in the manganites arise out of a doping-driven competition between energetically similar ground states, investigated doped multiferroics as a new example of this generic concept of phase competition. The results were the observation of an electronic conductor–insulator transition by control of band-filling in Ca-doped $BiFeO_3$. Application of electric fields enabled researchers to control and manipulate this electronic transition to the extent that a p–n junction can be created, erased and inverted in this material. A 'dome-like' feature in the doping dependence of the ferroelectric transition is observed around a Ca concentration of 1/8, where a new pseudo-tetragonal phase appears and the electric modulation of conduction is optimized [Fig. 10(a)]. c-AFM images [Fig. 10(b)] reveal that upon application of an electric field the material becomes conducting and that subsequent application of electric fields can reversibly turn the effect on and off. It has been proposed that this observation could open the door to merging magnetoelectrics and magnetoelectronics at room temperature by combining electronic conduction with electric and magnetic degrees of freedom already present in the multiferroic $BiFeO_3$. Fig. 10(c) shows the quasi-non-volatile and reversible modulation of electric conduction accompanied by the modulation of the ferroelectric state. The mechanism of this modulation in Ca-doped $BiFeO_3$ is based on electronic conduction as a consequence of the naturally produced oxygen vacancies that act as donor impurities to compensate Ca acceptors and maintain a highly stable Fe^{3+} valence state. Soon after this report, Schiemer *et al.*[117] provided a detailed structural study of the full Ca-doped $BiFeO_3$ system. This study sheds light on the evolution of properties and structure in this complex series – including the development of new phases and the impact of this on ferroelectricity and magnetism.

Magnetism and magnetoelectricity in $BiFeO_3$

So far we have focused mostly on electronic properties in $BiFeO_3$, in this section we will focus on the recent advances in understanding magnetic order in this material. As discussed previously, the structure of $BiFeO_3$ can be characterized by two distorted perovskite blocks connected along their body diagonal or the pseudocubic <111> to build a rhombohedral unit cell, is a G-type antiferromagnet with the moments confined to a plane perpendicular to the <111>-polarization directions, and possesses symmetry that permits a small canting of the moments in the structure resulting in a weak ferromagnetic moment of the Dzyaloshinskii–Moriya type. Also recall that Ederer and Spaldin suggested that only one easy magnetization axis in the energetically degenerate 111-plane might be selected when one was to strain the material.[71] Thus, one critical question concerning magnetism in

multiferroics such as $BiFeO_3$ that is of both fundamental and technological importance, is how this order parameter develops with strain and size effects?

Using angle and temperature dependent dichroic measurements and photoemission spectromicroscopy (Fig. 11), Holcomb *et al.*[118] have discovered that the antiferromagnetic order in $BiFeO_3$ evolves and changes systematically as a function of thickness and strain. Lattice mismatch induced strain is found to break the easy-plane magnetic symmetry of the bulk and leads to an easy axis of magnetization which can be controlled *via* the sign of the strain – 110-type for tensile strain and 112-type for compressive strain. This understanding of the evolution of magnetic structure and the ability to manipulate the magnetism in this model multiferroic has significant implications for eventual utilization of such magnetoelectric materials in applications.

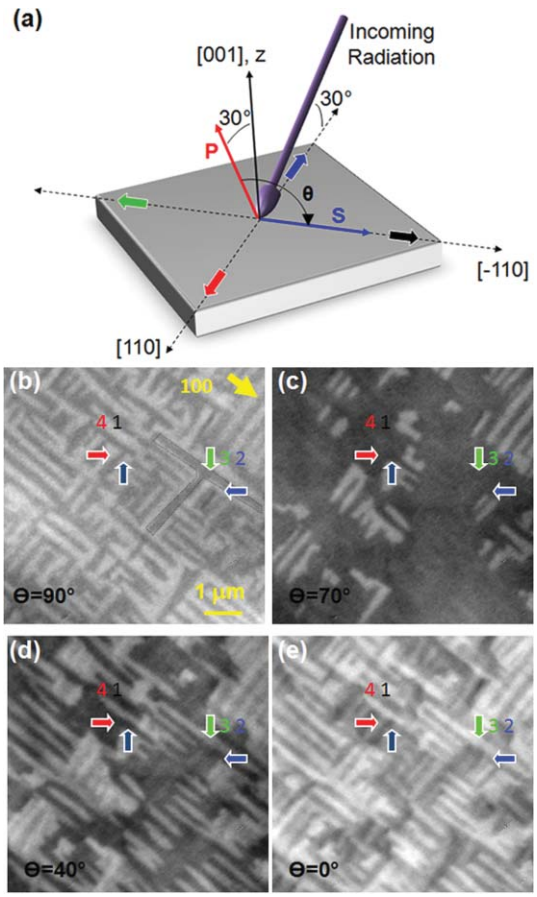

Fig. 11 (a) Schematic illustrating the experimental geometries used to probe the angle dependent linear dichroism in $BiFeO_3$. Photoemission electron microscopy images of $BiFeO_3$ at several angles of the electric vector of incident linear polarization α. The outlined arrows show the in-plane projection of the four ferroelectric directions. Images of domain structures taken at (b) $\alpha = 90°$, (c) $\alpha = 70°$, (d) $\alpha = 40°$, and (e) $\alpha = 0°$ (adapted from ref. 118).

At the same time, a number of recent findings are poised to definitively answer the questions surrounding the wide array of magnetic properties observed in $BiFeO_3$ thin films. There is now a growing consensus that epitaxial films (with a thickness less than ~100 nm) are highly strained and thus the crystal structure is more akin to a monoclinic phase rather than the bulk rhombohedral structure. Furthermore, a systematic dependence of the ferroelectric domain structure in the film as a function of the growth rate has been observed.[119] Films grown very slowly (for example by MBE, laser-MBE, or off-axis sputtering) exhibit a classical stripe-like domain structure that is similar to ferroelastic domains in tetragonal $Pb(Zr_x,Ti_{1-x})O_3$ films. Due to symmetry considerations, two sets of such twins are observed. These twins are made up of 71° ferroelastic walls, that form on the {101}-type planes (which is a symmetry plane). In contrast, if the films are grown rapidly (as was done in the original work of Wang *et al.*[17]) the domain structure is dramatically different. It now resembles a mosaic-like ensemble that consists of a dense distribution of 71°, 109° and 180° domain walls. It should be noted that 109° domain walls form on {001}-type planes (which is not a symmetry plane for this structure). Preliminary measurements reveal a systematic difference in magnetic moment between samples possessing different types and distributions of domain walls. The work of Martin *et al.*[119] suggests that such domain walls could play a key role in the many observations of enhanced magnetic moment in $BiFeO_3$ thin films.

This suggestion builds off of the work of Přívratská and Janovec,[120,121] where detailed symmetry analyzes were used to make the conclusion that magnetoelectric coupling could lead to the appearance of a net magnetization in the middle of antiferromagnetic domain walls. Specifically, they showed that this effect is allowed for materials with the *R*3*c* space group (*i.e.*, that observed for $BiFeO_3$). Although such analysis raises the possibility of such an effect, the group-symmetry arguments do not allow for any quantitative estimate of that moment. The idea that novel properties could occur at domain walls in materials presented by Přívratská and Janovec is part of a larger field of study of the morphology and properties of domains and their walls that has taken place over the last 50 years with increasing recent attention given to the study novel functionality at domain walls.[122–124] For instance, recent work has demonstrated that spin rotations across ferromagnetic domain walls in insulating ferromagnets can induce a local polarization in the walls of otherwise non-polar materials,[2,124] preferential doping along domain walls has been reported to induce 2D superconductivity in WO_{3-x}[125] and enhanced resistivity in phosphates,[126] while in paraelectric (non-polar) $SrTiO_3$ the ferroelastic domain walls appear to be ferroelectrically polarized.[127] Taking this idea one step further, Daraktchiev *et al.*[128,129] have proposed a thermodynamic (Landau-type) model with the aim of quantitatively estimating whether the walls of $BiFeO_3$ can be magnetic and, if so, to what extent they might contribute to the observed enhancement of magnetization in ultrathin films. One can develop a simple thermodynamic potential incorporating two order parameters expanded up to P^6 and M^6 terms (the transitions in $BiFeO_3$ are found experimentally to be first order, and the low-symmetry ($\pm P_0$, 0) phase is described here) with biquadratic coupling between the two order parameters (biquadratic coupling is always allowed by symmetry, and therefore always present in any system with two order parameters). Because biquadratic free energy terms such as P^2M^2 are scalars in any symmetry group, this potential can be written thus:

$$G_{MP} = G_0 + \frac{\kappa}{2}(\nabla P)^2 + \frac{\lambda}{2}(\nabla M)^2 + L_{MP}(P,M)$$
$$= G_0 + \frac{\kappa}{2}(\nabla P)^2 + \frac{\lambda}{2}(\nabla M)^2 + \frac{\alpha}{2}P^2 + \frac{\beta}{4}P^4 + \frac{\eta}{6}P^6 \quad (4)$$
$$+ \frac{a}{2}M^2 + \frac{b}{4}M^4 + \frac{n}{6}M^6 + \frac{\gamma}{2}P^2M^2$$

When one goes from $+P$ to $-P$, it is energetically more favorable for the domain wall energy trajectory not to go through the centre of the landscape ($P = 0$, $M = 0$), but to take a diversion through the saddle points at $M_0 \neq 0$, thus giving rise to a finite magnetization [Fig. 12]. The absolute values of the magnetic moment at the domain wall will depend on the values of the Landau coefficients as well as the boundary conditions imposed on the system, namely whether the material is magnetically ordered or not. Analysis of the phase space of this thermodynamic potential shows that it is possible for net magnetization to appear in the middle of ferroelectric walls even when the domains themselves are not ferromagnetic [Fig. 12(b)]. The authors of this model note, however, that it is presently only a ''toy model'' which does not take into account the exact symmetry of $BiFeO_3$, so it cannot yet quantitatively estimate how much domain walls can contribute to the magnetization. The exact theory of magnetoelectric coupling at the domain walls of BFO also remains to be formulated.

Recently, a holistic picture of the connection between processing, structure and properties has brought to light the role of magnetism at ferroelectric domain walls in determining the magnetic properties in $BiFeO_3$ thin films. By controlling domain structures through epitaxial growth constraints and probing these domain walls with exchange bias studies, X-ray magnetic dichroism based spectromicroscopy, and high-resolution transmission electron microscopy He *et al.*[130] have demonstrated that the formation of certain types of ferroelectric domain walls (*i.e.*, 109° walls) can lead to enhanced magnetic moments in $BiFeO_3$. Building off the work of Martin *et al.*,[119] the authors of this

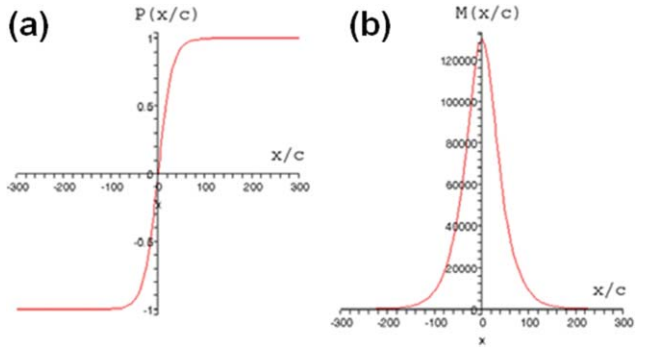

Fig. 12 Shape of (a) ferroelectric polarization and (b) magnetism across a domain wall in $BiFeO_3$ (adapted from ref. 128 and 129).

study were able to demonstrate that samples possessing 109° domain walls show significantly enhanced circular dichroism that is consistent with collective magnetic correlations, while samples with only 71° domain walls show no circular dichroism. In summary, it appears certain domain walls can give rise to enhanced magnetic behavior in $BiFeO_3$ thin films.

It is also important to note that Seidel *et al.*,[131] motivated by the desire to understand similar magnetic properties at domain walls in $BiFeO_3$, undertook a detailed scanning probe-based study of these materials and discovered a new and previously unanticipated finding: the observation of room temperature electronic conductivity at certain ferroelectric domain walls. The origin of the observed conductivity was explored using high resolution transmission electron microscopy and first-principles density functional computations. The results showed that domain walls in a multiferroic ferroelectric such as $BiFeO_3$, can exhibit unusual electronic transport behavior on a local scale that is quite different from that in the bulk of the material. Using a model (110)-oriented $BiFeO_3/SrRuO_3/SrTiO_3$ heterostructure with a smooth surface [Fig. 13(a)], the researchers were able to switch the $BiFeO_3$

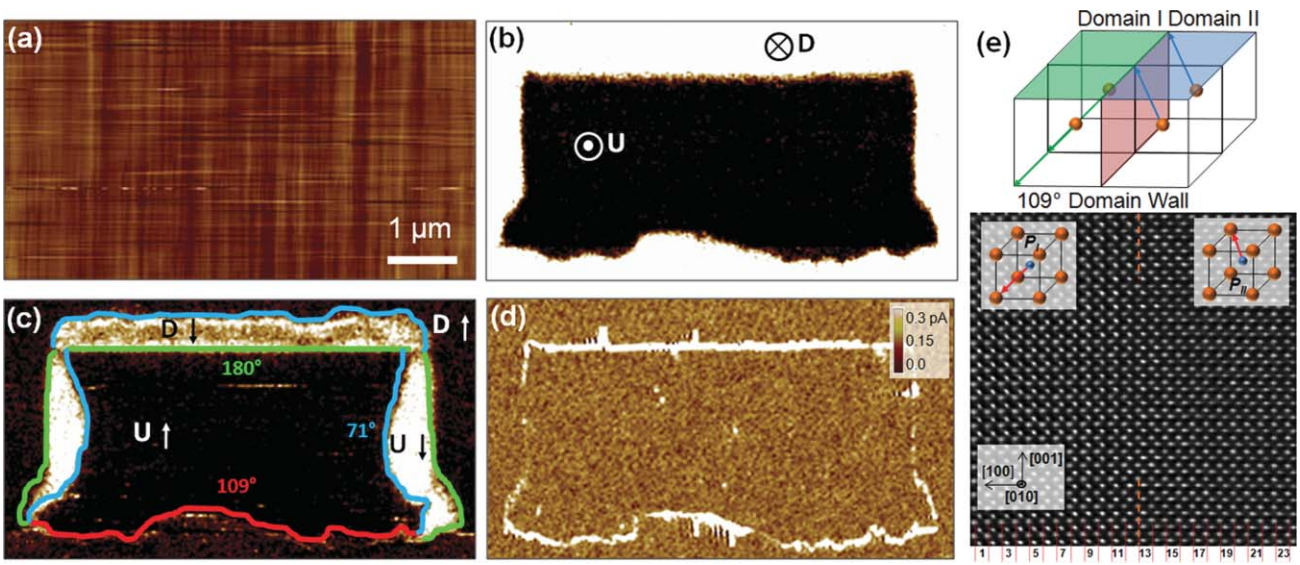

Fig. 13 Conduction at domain walls in $BiFeO_3$. (a) Topographic image of the surface of a model $BiFeO_3/SrRuO_3/SrTiO_3$ (110) sample. Corresponding (b) out-of-plane and (c) in-plane piezoresponse force microscopy image of an electrically poled region of this film. (d) Conducting-atomic force microscopy image reveals that 109° and 180° domain walls are conducting. (e) Schematic illustration of a 109° domain wall and a corresponding high-resolution transmission electron microscopy image of a 109° domain wall (adapted from ref. 131).

material is such a way that enabled them to create all the different types of domain walls possible in $BiFeO_3$ (*i.e.*, 71°, 109° and 180° domain walls) in a local region [Fig. 13(b) and (c)]. Conducting-atomic force microscopy (c-AFM) measurements [Fig. 13(d)] revealed conduction at 109° and 180° domain walls. Detailed high-resolution transmission electron microscopy studies [Fig. 13(e)] revealed this conductivity was, in part, structurally induced and can be activated and controlled on the scale of the domain wall width – about 2 nm in $BiFeO_3$. From the combined study of conductivity measurements, electron microscopy analysis, and density functional theory calculations, two possible mechanisms for the observed conductivity at the domain walls have been suggested: (1) an increased carrier density as a consequence of the formation of an electrostatic potential step at the wall; and/or (2) a decrease in the band gap within the wall and corresponding reduction in band offset with the c-AFM tip. It was noted that both possibilities are the result of structural changes at the wall and both may, in principle, be acting simultaneously, since they are not mutually exclusive.

Although many researchers anticipated strong magnetoelectric coupling in $BiFeO_3$, until the first evidence for this coupling in 2003 there was no definitive proof. Two years after this first evidence, a detailed report was published in which researchers observed the first visual evidence for electrical control of antiferromagnetic domain structures in a single phase multiferroic at room temperature. By combining X-ray photoemission electron microscopy (PEEM) imaging of antiferromagnetic domains [Fig. 14(a) and (b)] and piezoresponse force microscopy (PFM) imaging of ferroelectric domains [Fig. 14(c) and (d)] the researchers were able to observe direct changes in the nature of the antiferromagnetic domain structure in $BiFeO_3$ with application of an applied electric field [Fig. 14(e)].[132] This research showed that the ferroelastic switching events (*i.e.*, 71° and 109°) resulted in a corresponding rotation of the magnetization plane in $BiFeO_3$ [Fig. 14(f)] and has paved the way for further study of this material in attempts to gain room temperature control of ferromagnetism (to be discussed in detail later). This work has since been confirmed by neutron diffraction experiments in single-crystal $BiFeO_3$ as well.[133,134]

In this manuscript we have introduced the reader to the complex world of multiferroic materials. These exciting materials – that simultaneously possess multiple order parameters – have grabbed the attention of the materials science community over the last decade. The final impact of these materials on devices remains to be seen, but the possibilities are vast. In the meantime scientists and researchers are exploring the fundamental chemistry and physics of these materials. From the search for new multiferroic phases to the study of order parameter coupling to the design of systems that make use of the exotic functionalities of these materials the future

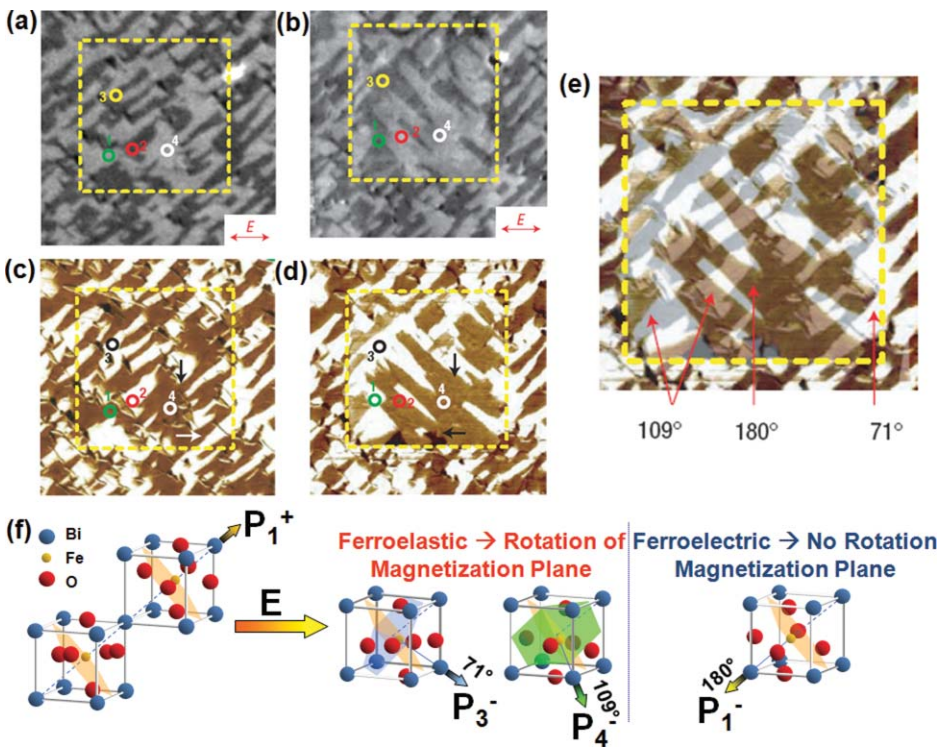

Fig. 14 Determination of strong magnetoelectric coupling in $BiFeO_3$. Photoemission electron microscopy (PEEM) images before (a) and after (b) electric field poling. The arrows show the X-ray polarization direction during the measurements. In-plane piezoresponse force microscopy images before (c) and after (d) electric field poling. The arrows show the direction of the in-plane component of ferroelectric polarization. Regions 1 and 2 (marked with green and red circles, respectively) correspond to 109° ferroelectric switching, whereas 3 (black and yellow circles) and 4 (white circles) correspond to 71° and 180° switching, respectively. In regions 1 and 2 the PEEM contrast reverses after electrical poling. (e) A superposition of in-plane PFM scans shown in c and d used to identify the different switching mechanisms that appear with different colors and are labeled in the figure (adapted from ref. 132). (f) Schematic illustration of coupling between ferroelectricity and antiferromagnetism in $BiFeO_3$. Upon electrically switching $BiFeO_3$ by the appropriate ferroelastic switching events (*i.e.*, 71° and 109° changes in polarization) a corresponding change in the nature of antiferromagnetism is observed (adapted from ref. 7).

of these materials is rich with possibility. Whether researchers are working to gain electric field control of ferromagnetism[135] or searching for the next candidate multiferroic material it is essential to understand and control the basic chemical nature of these materials. We have focused in this manuscript predominantly on one material – $BiFeO_3$ – but the lessons learned here extend to all multiferroics. Only by carefully controlling and understanding the materials chemistry can be achieve the results we set out to obtain.

References

1 R. Ramesh and N. A. Spaldin, *Nat. Mater.*, 2007, **6**, 21.
2 S.-W. Cheong and M. Mostovoy, *Nat. Mater.*, 2007, **6**, 13.
3 L. W. Martin, Y.-H. Chu and R. Ramesh, *Mater. Sci. Eng., R*, 2010, **68**, 89.
4 H. Schmid, *Ferroelectrics*, 1994, **162**, 665.
5 M. Fiebig, *J. Phys. D: Appl. Phys.*, 2005, **38**, R123.
6 W. Prellier, M. P. Singh and P. Murugavel, *J. Phys.: Condens. Matter*, 2005, **17**, R803.
7 L. W. Martin, S. P. Crane, Y.-H. Chu, M. B. Holcomb, M. Gajek, M. Huijben, C.-H. Yang, N. Balke and R. Ramesh, *J. Phys.: Condens. Matter*, 2008, **20**, 434220.
8 W. Eerenstein, N. D. Mathur and J. F. Scott, *Nature*, 2006, **442**, 759.
9 D. I. Khomskii, *J. Magn. Magn. Mater.*, 2006, **306**, 1.
10 J. B. Goodenough, J. M. Longo, in *Landolt-Börnstein, Numerical Data and Functional Relationships in Science and Technology, New Series*, Springer, Berlin, 1970, vol. III.4, pp. 126.
11 T. Mitsui, E. Nakamura, Y. Shiozaki, in *Landolt-Börnstein, Numerical Data and Functional Relationships in Science and Technology, New Series*, Springer, Berlin, 1981, vol. 16(1), pp. 126.
12 N. A. Hill, *J. Phys. Chem. B*, 2000, **104**, 6694.
13 N. A. Hill and N. Filippetti, *J. Magn. Magn. Mater.*, 2002, **242–245**, 976.
14 U. Opik and M. H. L. Pryce, *Proc. R. Soc. London, Ser. A*, 1957, **238**, 425.
15 P. S. Halasyamani and K. R. Poeppelmeier, *Chem. Mater.*, 1998, **10**, 2753.
16 D. Khomskii, *Physics*, 2009, **2**, 20.
17 J. Wang, J. B. Neaton, H. Zheng, V. Nagarajan, S. B. Ogale, B. Liu, D. Viehland, V. Vaithyanathan, D. G. Schlom, U. V. Waghmare, N. A. Spaldin, K. M. Rabe, M. Wuttig and R. Ramesh, *Science*, 2003, **299**, 1719.
18 A. M. dos Santos, A. Parashar, A. R. Raju, Y. S. Zhao, A. K. Cheetham and C. N. R. Rao, *Solid State Commun.*, 2002, **122**, 49.
19 T. Atou, H. Chiba, K. Ohoyama, Y. Yamaguichi and Y. Syono, *J. Solid State Chem.*, 1999, **145**, 639.
20 R. V. Shpanchenko, V. V. Chernaya, A. A. Tsirlin, P. S. Chizhov, D. E. Sklovsky and E. V. Antipov, *Chem. Mater.*, 2004, **16**, 3267.
21 A. A. Belik, M. Azuma, T. Saito, Y. Shimakawa and M. Takano, *Chem. Mater.*, 2005, **17**, 269.
22 L. W. Martin, Q. Zhan, Y. Suzuki, R. Ramesh, M. Chi, N. Browning, T. Mizoguchi and J. Kreisel, *Appl. Phys. Lett.*, 2007, **90**, 062903.
23 A. Kumar, L. W. Martin, S. Denev, J. B. Kortright, Y. Suzuki, R. Ramesh and V. Gopalan, *Phys. Rev. B*, 2007, **75**, 060101(R).
24 R. Seshadri and N. A. Hill, *Chem. Mater.*, 2001, **13**, 2892.
25 A. P. Levanyuk and D. G. Sannikov, *Sov. Phys. Usp.*, 1974, **17**, 199.
26 B. B. van Aken, T. T. M. Palstra, A. Filippetti and N. A. Spaldin, *Nat. Mater.*, 2004, **3**, 164.
27 J. Kreisel and N. Kenselmann, *Europhys. News*, 2009, **40**, 17.
28 N. Ikeda, H. Ohsumi, K. Ohwada, K. Ishii, T. Inami, K. Kakurai, Y. Murakami, K. Yoshii, S. Mori, Y. Horibe and H. Kito, *Nature*, 2005, **436**, 1136.
29 E. J. Verwey and P. W. Haayman, *Physica*, 1941, **8**, 979.
30 D. V. Efremov, J. Van Den Brink and D. I. Khomskii, *Nat. Mater.*, 2006, **5**, 937.
31 T. Kimura, T. Goto, H. Shintani, K. Ishizaka, T. Arima and Y. Tokura, *Nature*, 2003, **426**, 55.
32 N. Hur, S. Park, P. A. Sharma, J. S. Ahn, S. Guha and S.-W. Cheong, *Nature*, 2004, **429**, 392.
33 M. Kenzelmann, A. B. Harris, S. Jonas, C. Broholm, J. Schefer, S. B. Kim, C. L. Zhang, S.-W. Cheong, O. P. Vajk and J. W. Lynn, *Phys. Rev. Lett.*, 2005, **95**, 087206.
34 I. E. Dzyaloshinskii, *Sov. Phys. JETP*, 1957, **5**, 1259.
35 T. Moriya, *Phys. Rev.*, 1960, **120**, 91.
36 G. Lawes, A. B. Harris, T. Kimura, N. Rogado, R. J. Cava, A. Aharony, O. Entin-Wohlman, T. Yildirim, M. Kenzelmann and A. P. Ramirez, *Phys. Rev. Lett.*, 2005, **95**, 087205.
37 P. Curie, *J. Physique*, 1894, **3**, 393.
38 D. N. Astov, *Sov. Phys. JETP*, 1960, **11**, 708; D. N. Astov, *Sov. Phys. JETP*, 1961, **13**, 729.
39 G. T. Rado and V. J. Folen, *Phys. Rev. Lett.*, 1961, **7**, 310; V. J. Folen, G. T. Rado and E. W. Stalder, *Phys. Rev. Lett.*, 1961, **6**, 607.
40 V. E. Wood and A. E. Austin, *Int. J. Magn.*, 1973, **5**, 303.
41 M. Fiebig, *J. Phys. D: Appl. Phys.*, 2005, **38**, R123.
42 L. D. Landau, E. M. Lifshiftz, *Electrodynamics of Continuous Media*, Pergamon, Oxford, 1960.
43 T. H. O'Dell, *Electrodynamics of Magneto-Electric Media*, North-Holland, Amsterdam, 1970.
44 R. R. Birss, *Symmetry and Magnetism*, North-Holland, Amsterdam, 1966.
45 J. P. Rivera, *Ferroelectrics*, 1994, **161**, 165.
46 G. A. Smolensky, V. A. Ioffe, Commun. No. 71, *Colloque International du Magnetisme*, Grenoble, 1958.
47 G. A. Smolensky, A. I. Agranovskaya and V. A. Isupov, *Sov. Phys. Solid State*, 1959, **1**, 149.
48 N. A. Spaldin and M. Fiebig, *Science*, 2005, **309**, 391.
49 M. Eibschütz and H. J. Guggenheim, *Solid State Commun.*, 1968, **6**, 737.
50 J. F. Scott, *Ferroelectrics*, 1980, **24**, 127.
51 Y. N. Venevtsev, V. V. Gagulin and I. D. Zhitomirsky, *Ferroelectrics*, 1987, **73**, 221.
52 Y. Y. Tomashpol'ski, Y. N. Venevtsev and V. N. Beznozdrev, *Fiz. Tverd. Tela.*, 1965, **7**, 2763.
53 E. Ascher, H. Schmid and D. Tar, *Solid State Commun.*, 1964, **2**, 45.
54 H. Schmid, H. Rieder and E. Ascher, *Solid State Commun.*, 1965, **3**, 327.
55 A. V. Kovalev and G. T. Andreeva, *C. R. Acad. Sci.*, 1963, **256**, 1958.
56 P. Coeuré, F. Guinet, J. C. Peuzin, G. Buisson, E. F. Bertaut, *Proc. Int. Meeting Ferroelectricity*, Prague, 1966.
57 E. F. Bertaut and M. Mercier, *Phys. Lett.*, 1963, **5**, 27.
58 H. Sugie, N. Iwata and K. Kohn, *J. Phys. Soc. Jpn.*, 2002, **71**, 1558.
59 P. Royen and K. Swars, *Angew. Chem.*, 1957, **69**, 779.
60 F. Kubel and H. Schmid, *Acta Crystallogr., Sect. B: Struct. Sci.*, 1990, **46**, 698.
61 S. V. Kiselev, R. P. Ozerov and G. S. Zhdanov, *Sov. Phys. Dokl.*, 1963, **7**, 742.
62 J. R. Teague, R. Gerson and W. J. James, *Solid State Commun.*, 1970, **8**, 1073.
63 C. Michel, J. M. Moreau, G. D. Achenbach, R. Gerson and W. J. James, *Solid State Commun.*, 1969, **7**, 701.
64 J. M. Moreau, C. Michel, R. Gerson and W. J. James, *J. Phys. Chem. Solids*, 1971, **32**, 1315.
65 C. Tabares-Muños, J. P. Rivera, A. Bezinge, A. Monnier and H. Schmid, *Jpn. J. Appl. Phys.*, 1985, **24**, 1051.
66 F. Zavaliche, S. Y. Yang, T. Zhao, Y.-H. Chu, M. P. Cruz, C. B. Eom and R. Ramesh, *Phase Transitions*, 2006, **79**, 991.
67 P. Fischer, M. Polomska, I. Sosnowska and M. Szymanski, *J. Phys. C: Solid State Phys.*, 1980, **13**, 1931.
68 I. Sosnowska, T. Peterlin-Neumaier and E. Steichele, *J. Phys. C: Solid State Phys.*, 1982, **15**, 4835.
69 D. Lebeugle, D. Colson, A. Forget, M. Viret, P. Bonville, J. F. Marucco and S. Fusil, *Phys. Rev. B: Condens. Matter Mater. Phys.*, 2007, **76**, 024116.
70 J. B. Neaton, C. Ederer, U. V. Waghmare, N. A. Spaldin and K. M. Rabe, *Phys. Rev. B: Condens. Matter Mater. Phys.*, 2005, **71**, 014113.
71 C. Ederer and N. A. Spaldin, *Phys. Rev. B*, 2005, **71**, 060401(R).
72 W. Eerenstein, F. D. Morrison, J. Dho, M. G. Blamire, J. F. Scott and N. D. Mathur, *Science*, 2005, **307**, 1203a.
73 H. Béa, M. Bibes, S. Fusil, K. Bouzehouane, E. Jacquet, K. Rode, P. Bencok and A. Barthélémy, *Phys. Rev. B: Condens. Matter Mater. Phys.*, 2006, **74**, 020101.
74 J. Wang, A. Scholl, H. Zheng, S. B. Ogale, D. Viehland, D. G. Schlom, N. A. Spaldin, K. M. Rabe, M. Wuttig, L. Mohaddes, J. Neaton, U. Waghmare, T. Zhao and R. Ramesh, *Science*, 2005, **307**, 1203b.
75 F. Gao, X. Chen, K. Yin, S. Dong, Z. Ren, F. Yuan, T. Yu, Z. Zou and J. M. Liu, *Adv. Mater.*, 2007, **19**, 2889.

76 C. Tabares-Muñoz, J.-P. Rivera, A. Bezinges, A. Monnier and H. Schmid, *Jpn. J. Appl. Phys.*, 1985, **24**(Suppl. 24-2), 1051.
77 C. Tabares-Muñoz, Ph.D. Thesis, No. 2191, Université de Genève, 1986.
78 F. Kubel and H. Schmid, *J. Cryst. Growth*, 1993, **129**, 515.
79 D. N. Rakov, V. A. Murashov, A. A. Bush and Y. N. Venetsev, *Kristallografiya*, 1988, **33**, 445.
80 D. Lebeugle, D. Colson, A. Forget, M. Viret, P. Bonville, J. F. Marucco and S. Fusil, *Phys. Rev. B: Condens. Matter Mater. Phys.*, 2007, **76**, 024116.
81 S. Lee, T. Choi, W. Ratcliff, II, R. Erwin, S.-W. Cheong and V. Kiryukhin, *Phys. Rev. B*, 2008, **78**, 100101(R).
82 M. K. Singh, W. Prellier, M. P. Singh, R. S. Katiyar and J. F. Scott, *Phys. Rev. B: Condens. Matter Mater. Phys.*, 2008, **77**, 144403.
83 J. Kabelac, S. Ghosh, P. S. Dobal and R. Katiyar, *J. Vac. Sci. Technol., B*, 2007, **25**, 1049.
84 J. F. Ihlefeld, A. Kumar, V. Gopalan, D. G. Schlom, Y. B. Chen, X. Q. Pan, T. Heeg, J. Schubert, X. Ke, P. Schiffer, L. W. Martin, Y.-H. Chu and R. Ramesh, *Appl. Phys. Lett.*, 2007, **91**, 071922.
85 V. R. Palkar, J. John and R. Pinto, *Appl. Phys. Lett.*, 2002, **80**, 1628.
86 Y. H. Lee, C. C. Lee, Z. X. Liu, C. S. Liang and J. M. Wu, *Electrochem. Solid-State Lett.*, 2005, **8**, F55.
87 R. R. Das, D. M. Kim, S. H. Baek, F. Zavaliche, S.-Y. Yang, X. Ke, S. K. Streiffer, M. S. Rzchowski, R. Ramesh and C. B. Eom, *Appl. Phys. Lett.*, 2006, **88**, 242904.
88 S.-Y. Yang, F. Zavaliche, L. Mohaddes-Ardabili, V. Vaithyanathan, D. G. Schlom, Y. J. Lee, Y.-H. Chu, M. P. Cruz, T. Zhao and R. Ramesh, *Appl. Phys. Lett.*, 2005, **87**, 102903.
89 R. Ueno, S. Okaura, H. Funakubo and K. Saito, *Jpn. J. Appl. Phys.*, 2005, **44**, L1231.
90 S. K. Singh, Y. K. Kim, H. Funakubo and H. Ishiwara, *Appl. Phys. Lett.*, 2006, **88**, 062502.
91 J. Wang, H. Zheng, Z. Ma, S. Prasertchoung, M. Wuttig, R. Droopad, J. Yu, K. Eisenbeiser and R. Ramesh, *Appl. Phys. Lett.*, 2004, **85**, 2574.
92 W. Tian, V. Vaithyanathan, D. G. Schlom, Q. Zhan, S.-Y. Yang, Y.-H. Chu and R. Ramesh, *Appl. Phys. Lett.*, 2007, **90**, 172908.
93 Y.-H. Chu, T. Zhao, M. P. Cruz, Q. Zhan, P.-L. Yang, L. W. Martin, M. Huijben, C.-H. Yang, F. Zavaliche, H. Zheng and R. Ramesh, *Appl. Phys. Lett.*, 2007, **90**, 252906.
94 Y.-H. Chu, Q. Zhan, L. W. Martin, M. P. Cruz, P.-L. Yang, G. W. Pabst, F. Zavaliche, S.-Y. Yang, J.-X. Zhang, L.-Q. Chen, D. G. Schlom, I.-N. Lin, T.-B. Wu and R. Ramesh, *Adv. Mater.*, 2006, **18**, 2307.
95 Y.-H. Chu, M. P. Cruz, C.-H. Yang, L. W. Martin, P.-L. Yang, J.-X. Zhang, K. Lee, P. Yu, L.-Q. Chen and R. Ramesh, *Adv. Mater.*, 2007, **19**, 2662.
96 S. K. Streiffer, C. B. Parker, A. E. Romanov, M. J. Lefevre, L. Zhao, J. S. Speck, W. Pompe, C. M. Foster and G. R. Bai, *J. Appl. Phys.*, 1998, **83**, 2742.
97 Y.-H. Chu, Q. He, C.-H. Yang, P. Yu, L. W. Martin, P. Shafer and R. Ramesh, *Nano Lett.*, 2009, **9**, 1726.
98 Y.-H. Lee, J.-M. Wu and C.-H. Lai, *Appl. Phys. Lett.*, 2006, **88**, 042903.
99 X. Qi, J. Dho, R. Tomov, M. G. Blamire and J. L. MacManus-Driscoll, *Appl. Phys. Lett.*, 2005, **86**, 062903.
100 G. L. Yuan and S. W. Or, *Appl. Phys. Lett.*, 2006, **88**, 062905.
101 C. F. Chung, J. P. Lin and J. M. Wu, *Appl. Phys. Lett.*, 2006, **88**, 242909.
102 J. K. Kim, S. S. Kim, W.-J. Kim, A. S. Bhalla and R. Guo, *Appl. Phys. Lett.*, 2006, **88**, 132901.
103 Z. V. Gabbasova, M. D. Kuz'min, A. K. Zvezdin, I. S. Dubenko, V. A. Murashov, D. N. Rakov and I. B. Krynetsky, *Phys. Lett. A*, 1991, **158**, 491.
104 A. V. Zalesskii, A. A. Frolov, T. A. Khimich and A. A. Bush, *Phys. Solid State*, 2003, **45**, 141.
105 D. Lee, M. G. Kim, S. Ryu, H. M. Jang and S. G. Lee, *Appl. Phys. Lett.*, 2005, **86**, 222903.
106 Y.-H. Chu, Q. Zhan, M. P. Cruz, L. W. Martin, T. Zhao, P. Yu, R. Ramesh, P. T. Joseph, I. N. Lin, W. Tian and D. G. Schlom, *Appl. Phys. Lett.*, 2008, **92**, 102909.
107 D. H. Wang, W. C. Goh, M. Ning and C. K. Ong, *Appl. Phys. Lett.*, 2006, **88**, 212907.
108 V. A. Chomchenko, D. A. Kiselev, J. M. Vieira, A. L. Kholkin, M. A. Sa and Y. G. Pogorelov, *Appl. Phys. Lett.*, 2007, **90**, 242901.
109 S. Fujino, M. Murakami, V. Anbusathaiah, S.-H. Lim, V. Nagarajan, C. J. Fennie, M. Wuttig, L. Salamanca-Riba and I Takeuchi, *Appl. Phys. Lett.*, 2008, **92**, 202904.
110 C.-J. Cheng, D. Kan, S.-H. Lim, W. R. McKenzie, P. R. Munroe, L. G. Salamanca-Riba, R. L. Withers, I. Takeuchi and V. Nagarajan, *Phys. Rev. B: Condens. Matter Mater. Phys.*, 2009, **80**, 014109.
111 C.-J. Cheng, A. Y. Borisevich, D. Kan, I. Takeuchi and V. Nagarajan, *Chem. Mater.*, 2010, **22**, 2588.
112 D. Kan, L. Pálová, V. Anbusathaiah, C. J. Cheng, S. Fujino, V. Nagarajan, K. M. Rabe and I. Takeuchi, *Adv. Funct. Mater.*, 2010, **20**, 1108.
113 R. J. Zeches, M. D. Rossell, J. X. Zhang, A. J. Hatt, Q. He, C.-H. Yang, A. Kumar, C. H. Wang, A. Melville, C. Adamo, G. Sheng, Y.-H. Chu, J. F. Ihlefeld, R. Erni, C. Ederer, V. Gopalan, L. Q. Chen, D. G. Schlom, N. A. Spaldin, L. W. Martin and R. Ramesh, *Science*, 2009, **326**, 977.
114 A. J. Hatt, N. A. Spaldin and C. Ederer, *Phys. Rev. B: Condens. Matter Mater. Phys.*, 2010, **81**, 054109.
115 D. Mazumdar, V. Shelke, M. Iliev, S. Jesse, A. Kumar, S. V. Kalinin, A. P. Baddorf and A. Gupta, *Nano Lett.*, 2010, **10**, 2555.
116 C.-H. Yang, J. Seidel, S. Y. Kim, P. B. Rossen, P. Yu, M. Gajek, Y.-H. Chu, L. W. Martin, M. B. Holcomb, Q. He, P. Maksymovych, N. Balke, S. V. Kalinin, A. P. Baddorf, S. R. Basu, M. L. Scullin and R. Ramesh, *Nat. Mater.*, 2009, **8**, 485.
117 J. Schiemer, R. Withers, L. Norén, Y. Lin, L. Bourgeois and G. Stewart, *Chem. Mater.*, 2009, **21**, 4223.
118 M. B. Holcomb, L. W. Martin, A. Scholl, Q. He, P. Yu, C.-H. Yang, S. Y. Yang, P.-A. Glans, M. Valvidares, M. Huijben, J. B. Kortright, J. Guo, Y.-H. Chu and R. Ramesh, *Phys. Rev. B: Condens. Matter Mater. Phys.*, 2010, **81**, 134406.
119 L. W. Martin, Y.-H. Chu, M. B. Holcomb, M. Huijben, S. J. Han, D. Lee, A. Arenholz, S. X. Wang and R. Ramesh, *Nano Lett.*, 2008, **8**, 2050.
120 J. Přívratská and V. Janovec, *Ferroelectrics*, 1997, **204**, 321.
121 J. Přívratská and V. Janovec, *Ferroelectrics*, 1999, **222**, 23.
122 L. Thomas, M. Hayashi, X. Jiang, R. Moriya, C. Rettner and S. Parkin, *Science*, 2007, **315**, 1553.
123 V. Goltsev, R. V. Pisarev, Th. Lottermoser and M. Fiebig, *Phys. Rev. Lett.*, 2003, **90**, 177204.
124 M. Mostovoy, *Phys. Rev. Lett.*, 2006, **96**, 067601.
125 A. Aird and E. K. H. Salje, *J. Phys.: Condens. Matter*, 1998, **10**, L377.
126 M. Bartels, V. Hagen, M. Burianek, M. Getzlaff, U. Bismayer and R. Wiesendanger, *J. Phys.: Condens. Matter*, 2003, **15**, 957.
127 P. Zubko, G. Catalan, A. Buckley, P. R. L. Welche and J. F. Scott, *Phys. Rev. Lett.*, 2007, **99**, 167601.
128 M. Daraktchiev, G. Catalan and J. F. Scott, *Ferroelectrics*, 2008, **375**, 122.
129 G. Catalan and J. F. Scott, *Adv. Mater.*, 2009, **21**, 2463.
130 Q. He, M. Daraktchiev, G. Catalan, E. Arenholz, A. Scholl, A. Fraile-Rodriguez, S.-Y. Yang, C.-H. Yang, P. Yu, J. Wu, D. Lee, Z. Q. Qiu, S. X. Wang, Y.-H. Chu, J. F. Scott, L. W. Martin and R. Ramesh, *Nat. Mater.*, submitted.
131 J. Seidel, L. W. Martin, Q. He, Q. Zhan, Y.-H. Chu, A. Rother, M. E. Hawkridge, P. Maksymovych, P. Yu, M. Gajek, N. Balke, S. V. Kalinin, S. Gemming, F. Wang, G. Catalan, J. F. Scott, N. A. Spaldin, J. Orenstein and R. Ramesh, *Nat. Mater.*, 2009, **8**, 229.
132 T. Zhao, A. Scholl, F. Zavaliche, K. Lee, M. Barry, A. Doran, M. P. Cruz, Y.-H. Chu, C. Ederer, N. A. Spaldin, R. R. Das, D. M. Kim, S. H. Baek, C. B. Eom and R. Ramesh, *Nat. Mater.*, 2006, **5**, 823.
133 D. Lebeugle, D. Colson, A. Forget, M. Viret, A. M. Bataille and A. Gukasov, *Phys. Rev. Lett.*, 2008, **100**, 227602.
134 S. Lee, W. Ratcliff, S.-W. Cheong and V. Kiryukhin, *Appl. Phys. Lett.*, 2008, **92**, 192906.
135 Y.-H. Chu, L. W. Martin, M. B. Holcomb, M. Gajek, S.-J. Han, Q. He, N. Balke, C.-H. Yang, D. Lee, W. Hu, Q. Zhan, P.-L. Yang, A. Fraile-Rodriguez, A. Scholl, S. X. Wang and R. Ramesh, *Nat. Mater.*, 2008, **7**, 478.

